Journal of Magnetics 16(4), 363-367 (2011) http://dx.doi.org/10.4283/JMAG.2011.16.4.363

Programmable Magnetic Actuation of Biomolecule Carriers using NiFe Stepping Stones

Byunghwa Lim, Ilgyo Jeong, S. Anandakumar, K. W. Kim, and CheolGi Kim*

Department of Materials Science and Engineering, Chungnam National University, Daejeon 305-764, Korea

(Received 17 October 2011, Received in final form 14 November 2011, Accepted 14 November 2011)

We have designed, fabricated and demonstrated a novel micro-system for programmable magnetic actuation using magnetic elliptical pathways on Si substrates. Lithographically patterned soft NiFe ellipses are arranged sequentially perpendicular to each other as stepping stones for the transport of magnetic beads. We have measured the magnetization curve of the ellipsoid (9 μm × 4 μm × 0.1 μm) elements with respect to the long and short axes of the ellipse. We found that the magnetization in the long axis direction is larger than that in the short axis direction for an applied field of ≤ 1,000 Oe, causing a force on carriers that causes them to move from one element to another. We have successfully demonstrated a micro-system for the magnetic actuation of biomolecule carriers of superparamagnetic beads (Dynabead® 2.8 μm) by rotating the external magnetic field. This novel concept of magnetic actuation is useful for future integrated lab-on-a-chip systems for biomolecule manipulation, separation and analysis.

Keywords : magnetic pathways, magnetic beads, NiFe ellipse

1. Introduction

Magnetic actuation and programmable control of biomolecule carriers in microfluidic channels are important for chemical and biological analysis [1]. Since the micro size magnetic beads play an important role as carriers/labels of biomolecules, external control and programmable motion are prerequisites for biomolecule manipulation and analysis [2]. Microfluidic devices provide a platform for studying single cells or small populations of cells in ultralow media volumes. In general, microfluidic devices are passive systems which utilize fluidic behavior for manipulating biological cells within structures of micrometer dimensions; this is a field of study closely related to chemical cytometry [3]. On the other hand, active micro devices such as current carrying conductors, permanent magnets and electromagnets utilize magnetic forces for the manipulation of biomolecule carriers [4-9].

Although there are several existing technologies for the actuation and programmable control of magnetic beads, they have limited capability in performing complex manipulations of the magnetic beads. In general, these micro systems are made up of permanent magnets or electromagnets with dimensions of millimeter size and they generate small magnetic fields in the fluidic channels, which do not allow for magnetic fields localized over micro-scale regions. They are difficult and expensive to fabricate and also they generate heat, which may damage to biological entities in the channel [10].

On-chip soft magnetic micro structures are a different class of manipulation systems, which utilize external magnetic fields for control of the magnetic beads in the microfluidic channels [11]. These systems are less common in the literature compared to conventional manipulation systems. These systems are easier to fabricate and integrate with microfluidic channels; moreover there is no heat generation on-chip. In general, soft magnetic materials have saturation magnetization of the order of one Tesla, and if the magnetic geometry is designed such that the characteristic length scales are of the order of 100 μm or less, then the magnetic field gradients are in the range of 10^4 T/m.

In the year 2010, our group reported a method for translocation of bio-functionalized magnetic beads using continuously patterned soft magnetic semi-elliptical elements [12]. In the report we demonstrated obliquely patterned soft magnetic semi-elliptical magnetic pathways for the converging and diverging of bio-functionalized magnetic beads at the converging site. In the present work,

*Corresponding author: Tel: +82-42-821-6632
Fax: +82-42-822-6227, e-mail: cgkim@cnu.ac.kr

we have designed, fabricated and demonstrated a novel micro-system utilizing discretely patterned elliptical elements as pathways for programmable actuation of biomolecule carriers of superparamagnetic micro beads along the pathways with respect to an external rotating magnetic field in the fluidic channel.

2. Theoretical Background for Magnetic Force on a Magnetic Carrier Bead

The magnetic force on a magnetic bead is proportional to the product of the field strength and the gradient of the local magnetic field. The key parameter for the actuation of magnetic beads using soft magnetic microstructures is the creation of large local field gradients around the magnetic elements [13]. If the external magnetic field is large enough to magnetically saturate the superparamagnetic magnetic bead, then maximizing the force is equivalent to maximizing the magnetic field gradient. If we neglect the magnetic property of the suspension medium, the force acting on a magnetic bead is given as follows [14-16].

$$\vec{F} = \frac{1}{2}\frac{V\chi_{bead}}{\mu_0}\nabla B^2 \tag{1}$$

When a circular element is considered instead of an elliptical one in order to simplify the mathematical expression, equation (1) in polar coordinates (r, θ) is given as follows;

$$F = F_r\hat{r} + F_\theta\hat{\theta}$$
$$= \frac{\chi_v V}{\mu_0}\left[\left(B_r\frac{\partial B_r}{\partial r} + B_\theta\frac{\partial B_\theta}{\partial r}\right)r + \frac{1}{r}\left(B_r\frac{\partial B_r}{\partial \theta} + B_\theta\frac{\partial B_\theta}{\partial \theta}\right)\hat{\theta}\right] \tag{2}$$

Here, F_r, F_θ are the force components in the radial and angular rotational directions, respectively, and B_r, B_θ are the radial and angular components of the magnetic field, respectively.

Without the exact mathematical expressions for B_r and B_θ, it is qualitatively noted that a bead subjected to a rotational magnetic field rotates along the edge of the pattern with its rotation synchronized with the field rotation, as schematically shown in Fig. 1(a), due to the rotational force component in equation (2). The movement of the bead from element A to neighbouring element B, as schematically shown in Fig. 1(b), is governed by the radial forces between two elements at points P_a and P_b. When the magnetic field B at P_a and P_b is assumed to be proportional to the magnetization M of each element, A and B, respectively, the force is approximately dependent on M^2 at each point from equation (2).

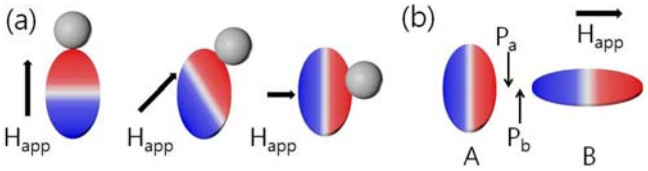

Fig. 1. (Color online) Schematic drawing of carrier movement: (a) rotation in a pattern, (b) trans-moving from element A to neighbouring element B.

3. Experiment

3.1. Fabrication of magnetic pathways

The soft magnetic NiFe elliptical magnetic pathways were patterned on the silicon substrate by using conventional photolithography and lift-off techniques. The process is shown schematically in Fig. 2. Firstly, the patterns were drawn using AutoCAD software and a chromium metal mask of the desired pattern is created by conventional electron beam lithography and used to mask the pattern on the Si substrate. Using the metal mask, an inverse image is created on the photoresist layer coating of the Si wafer using a mask aligner. The sample is exposed to UV light through the metal mask and then rinsed with developer and DI water to stencil the pattern onto the photoresist-coated wafer.

A thin layer of NiFe film (100 nm) was deposited over the patterned area on the Si wafer using a sputtering process. After the permalloy ($Ni_{80}Fe_{20}$) layer has been deposited, the wafer is immersed in acetone, which can dissolve the photoresist layer. Once the photoresist is dissolved by the liquid, the NiFe layer over it gets 'lifted off', leaving the NiFe patterns that were deposited onto the substrate itself, which forms the final pattern on the wafer [17].

3.2. Magnetic bead monitoring setup

The control of superparmagnetic beads along the elliptical pathway in the fluidic cell was conducted in a quasi-hydrostatic environment. The fluidic cell of 1 × 1 × 0.2

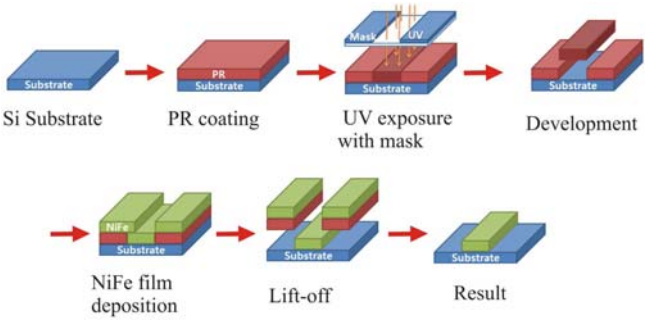

Fig. 2. (Color online) Photolithography and lift-off process for patterning the magnetic pathway.

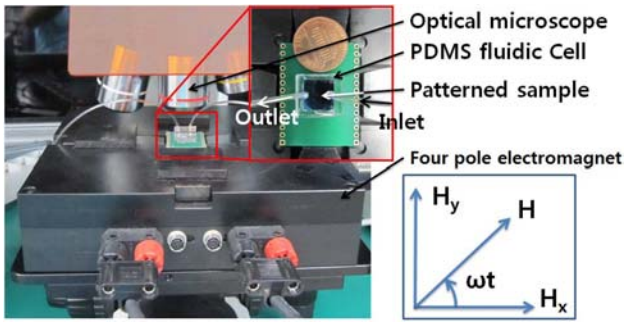

Fig. 3. (Color online) Experimental setup for bead placement, including a rotating external magnetic field, the fluid cell containing the patterned sample, and an optical microscope connected to a CCD camera to study the magnetic bead movement on the NiFe elliptical pathways.

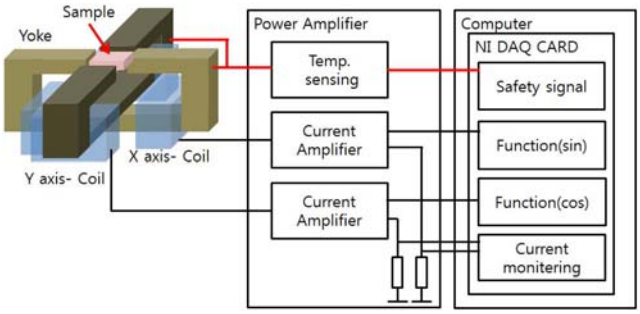

Fig. 4. (Color online) Block diagram of rotating magnetic field system with integrated x-y ferrite core solenoids.

cm^3 was fabricated using polydimethylsiloxane (PDMS) to keep the solution on the silicon substrate, and covered with a glass slide. A system for injecting the diluted magnetic beads solution into the fluidic cell was arranged by tubing the inlet and outlet of the fluidic cell. A weak flow of the suspension was used to trap magnetic beads near the elliptical elements. The motion of the magnetic beads on the pathways was observed through an optical microscope connected with a computer, as shown in Fig. 3.

3.3. Rotating magnetic field for magnetic force

The driving force for the magnetic bead motion on an elliptical pathway was achieved by the rotational magnetic field. The rotating magnetic field was produced by ferrite core solenoids which were arranged along mutually orthogonal axes (x-y) with respect to the wafer surface, as shown in Fig. 4. Two current sources were controlled by Labview software to supply sinusoidal waveforms to each solenoid coil. The current sources along the orthogonal axes were adjusted to have a 90° phase difference, as $\vec{H}_x = \vec{i}\cos(\omega t)$ and $\vec{H}_y = \vec{j}\sin(\omega t)$, in order to generate a rotating magnetic field in the x-y plane. The maximum field of 7.9 kAm^{-1} can be obtained by applying 2 A of current to each of the ferrite core solenoids [12].

4. Results and Discussion

4.1. Directional magnetization of elliptical elements

As stated in section II, the trans-moving actuation of magnetic bead carriers is dependent on the direction of magnetization of the elliptical element. The inset of Fig. 5(a) shows the lithographically patterned NiFe (9 μm × 4 μm × 0.1 μm) ellipse elements for measuring the directional magnetization, of which the dimensions are the same as those of the pathway element. For the maximum magnetic field ranges of ± 3,000 Oe, and ± 100 Oe, respectively, Fig. 5(a), (b) show the normalized magnetization of the patterns measured along the long and short axis directions by vibrating sample magnetometer (VSM). The saturation field is ~5 Oe for a 0.1 μm thick thin film, as shown in Fig. 5(c). However, the saturation fields in the long and short axis directions are 500 Oe and 2000 Oe, respectively, due to a smaller demagnetization factor in the long axis direction than that of the short axis direction. It is clearly evident that the magnetization in

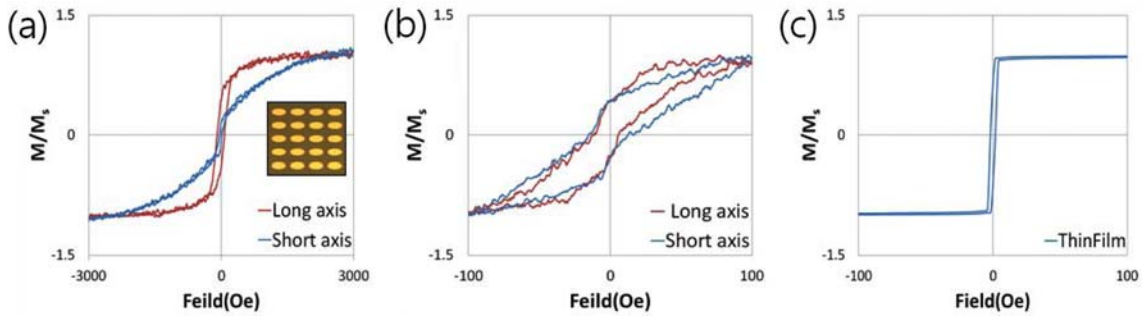

Fig. 5. (Color online) Magnetization curves of the elements measured in the long and short axis directions. Inset: lithographically patterned NiFe ellipse elements (9 μm × 4 μm × 0.1 μm) for the applied field ranges of ± 3,000 Oe (a), and ± 100 Oe (b); (c) magnetization curve for 0.1 μm thick thin film.

the long axis direction in larger than that in the short axis direction for an applied field ≤ 1,000 Oe. With larger magnetization in the long axis direction, it is noted that the carrier bead in element A in Fig. 1(b) will trans-move to element B by considering the force between elements A and B via equation (2).

4.2. Actuation of carrier along stepping stone elements

Fig. 6 shows the discretely arranged elliptical pathways. When an external magnetic field (~100 Oe) is applied, the superparamagnetic beads will be magnetized partially and attracted to the fully saturated poles of the NiFe elements, where stronger stray fields will be produced in alignment with their long axes and weaker stray fields with their short axes.

As shown in Fig. 6(a-f), we have demonstrated the motion of magnetic beads (Dynabead®M 280) of size 2.8 μm [18] on the patterned NiFe elliptical pathways. The inhomogeneous stray magnetic fields will govern the motion of the magnetic bead along the elliptical magnetic pathways. When rotating the magnetic field in the clockwise direction, the magnetic bead moves around the perimeter of the NiFe ellipses and jumps from one ellipse to another.

4.3. Linear transport of chain of magnetic beads

We demonstrated the linear transport of a chain of magnetic beads using elliptical magnetic pathways as shown in Fig. 6(a-f). For this experiment, we firstly prepared a chain of magnetic beads by applying an external magnetic field to the diluted magnetic bead solution. When a high magnetic field is applied, the superparamagnetic magnetic beads get attracted to each other due to dipolar interactions between the magnetic beads and form a chain of magnetic beads. Later, we injected the chain of beads into the fluidic channel under a magnetic field containing

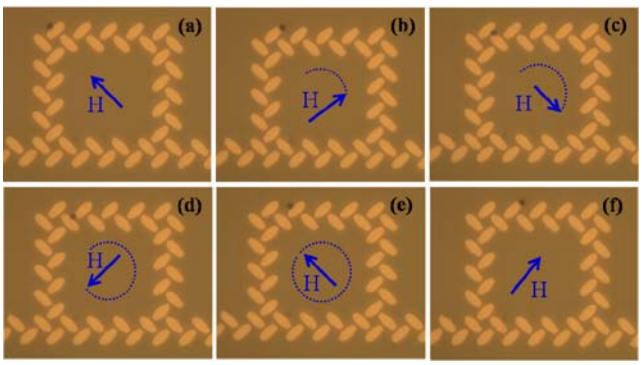

Fig. 6. (Color online) (a-f) Magnetic beads jump from one ellipse to another as the external magnetic field rotates in the clock wise direction.

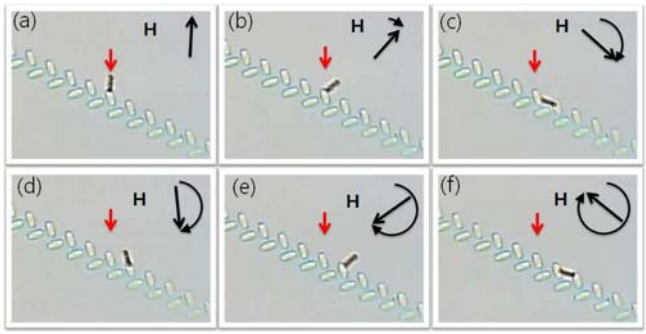

Fig. 7. (Color online) (a-f) Linear transport of a chain of magnetic beads with respect to the external rotating magnetic field.

elliptical magnetic patterned pathways. The chains of magnetic beads are attracted immediately to the saturated poles of the magnetic elliptical elements. The linear transport of the chain of magnetic beads was observed through an optical microscope by rotating the external magnetic field in the clockwise direction. As show in Fig. 7(a-f) the chain of magnetic beads jumps from one ellipse to another ellipse along the pathway as the external magnetic field rotates in the clockwise direction.

5. Conclusion

We have successfully designed, fabricated and demonstrated a novel micro-system for the magnetic actuation of biomolecule carriers of superparamagnetic micro beads (Dynabead®M 280) on discretely patterned soft magnetic elliptical magnetic pathways. Lithographically patterned soft NiFe ellipses (9 μm × 4 μm × 0.1 μm) are arranged sequentially orthogonal to each other as pathways for the transport of magnetic beads. The magnetization curve of the ellipsoid (9 μm × 4 μm × 0.1 μm) elements with respect to the long and short axis of the ellipse is measured and it is found that the magnetization in long axis direction is larger than that in the short axis direction for an applied field of ≤ 1,000 Oe, causing a force which drives the movement of carriers from one element to another. The generation of inhomogeneous stray fields on the magnetic pathway governs the motion of the magnetic beads with respect to the rotating magnetic field. Also, we have demonstrated linear transport of a chain of magnetic beads on the elliptical pathways, which can be a useful technique for the translocation of biomolecule carriers with a high aspect ratio. The versatility in the design of magnetic pathways safeguards a precision control of the magnetic beads with respect to the external rotating magnetic fields. This system provides a new platform for future biomolecule separation and manipulation by using

magnetic beads on a single chip.

Acknowledgement

This study was financially supported by the research fund of Chungnam National University in 2010.

References

[1] I. Safarik, M. Safarikova, and J. Chormatogr. B: Biomed. Appl. **722**, 33 (1999).
[2] M. A. M. Gijs, Microfluid Nanofluid **1**, 22 (2004).
[3] R. N. Zare and S. Kim, Annu. Rev. Biomed. Eng. **12**, 187 (2010).
[4] T. Deng, G. M. Whiteside, M. Radhakrishnan, G. Zabow, and M. Prentiss, Appl. Phys. Lett. **78**, 1775 (2001).
[5] A. Rida, V. Fernanadez, and M. A. M. Gijs, Appl. Phys. Lett. **83**, 2396 (2003).
[6] Q. Ramadan, C. Yu, V. Samper, and D. P. Poenar, Appl. Phys. Lett. **88**, 032501 (2006).
[7] E. Mirowski, J. Moreland, A. Zhang, S. E. Russek, and M. J. Donahue, Appl. Phys. Lett. **86**, 243901 (2005).
[8] T. Deng, M. Prentiss, and G. M. Whitesides, Appl. Phys. Lett. **80**, 461 (2002).
[9] E. Mirowski, J. Moreland, S. Russek, M. Donahue, and K. Hsieh, J. Magn. Magn. Mater. **311**, 401 (2007).
[10] K. Smistrup, T. Lund-Olesen, M. F. Hansen, and P. T. Tang, J. Appl. Phys. **99**, 08P102 (2006).
[11] K. Gunnarsson, P. E. Roy, S. Felton, J. Pihl, P. Svedlindh, S. Berner, H. Lidbaum, and S. Oscarsson, Adv. Mater. **17**, 1730 (2005).
[12] S. Anandakumar, V. Sudha Rani, Sunjong Oh, B. L. Sinha, M. Takahashi, and C. G. Kim, Biosens. Bioelectron. **26**, 1755 (2010).
[13] R. Wirix-Speetjens and J. de Boek, IEEE Trans. Magn. **41**, 1944 (2004).
[14] M. Zborowski, C. B. Fuh, R. Green, L. Sun, and J. J. Chalmers, Anal. Chem. **67**, 3702 (1995).
[15] Q. Ramadan, V. Samper, D. P. Poenar, and C. Yu, Biosens. Bioelectron. **21**, 1693 (2006).
[16] N. Pamme, Lab Chip. **6**, 24 (2006).
[17] S. Anandakumar, V. Sudha Rani, J.-R. Jeong, C. G. Kim, K. W. Kim, and B. Parvatheeswara Rao, J. Appl. Phys. **105**, 07B312 (2009).
[18] http://www.dynalbiotech.com